Case Studies in Thermal Engineering 60 (2024) 104760

Contents lists available at ScienceDirect

Case Studies in Thermal Engineering

journal homepage: www.elsevier.com/locate/csite

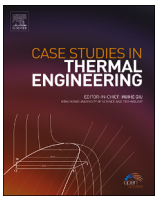

Performance of proton exchange membrane fuel cell system by considering the effects of the gas diffusion layer thickness, catalyst layer thickness, and operating temperature of the cell

Sajad Hamedi [a], Ali Basem [b, **], Murtadha M. Al-Zahiwat [c], Ahmed Khudhair AL-Hamairy [d], Dheyaa J. Jasim [e], Soheil Salahshour [f, g, h], Sh. Esmaeili [i, *]

[a] Engineering Mechanics Department, Virginia Tech University, Blacksburg, Virginia, USA
[b] Faculty of Engineering, Warith Al-Anbiyaa University, Karbala, 56001, Iraq
[c] Department of Chemical engineering, College of Engineering, University of Misan, Amarah, Iraq
[d] Anesthesia Techniques Department, College of Health and Medical Techniques, Al-Mustaqbal University, 51001, Babylon, Iraq
[e] Department of Petroleum Engineering, Al-Amarah University College, Maysan, Iraq
[f] Faculty of Engineering and Natural Sciences, Istanbul Okan University, Istanbul, Turkey
[g] Faculty of Engineering and Natural Sciences, Bahcesehir University, Istanbul, Turkey
[h] Department of Computer Science and Mathematics, Lebanese American University, Beirut, Lebanon
[i] Faculty of Physics, Semnan University, P.O. Box: 35195-363, Semnan, Iran

HIGHLIGHTS

- Effect of the cross-section shape of the cathode and anode channel of the PEMFC is investigated.
- Amount of pressure drop is much lower than the channel with a length of 150 mm.
- In these thicknesses, the current density is increased and less space is occupied.
- Pressure and temperature in the catalyst layer of the cathode side are greater than the anode.
- Temperature in the central regions of the catalyst layer is higher than the lateral regions.

ARTICLE INFO

Keywords:
PEM fuel cell
Trapezoidal channel
Single-phase
Structural characteristics

ABSTRACT

Background: In this research, the effect of anode and cathode channel cross-sectional shape on the performance of PEM fuel cell was investigated and the appropriate length and dimensions of the channel were determined. Finally, for the determined geometric conditions, the cell performance at different voltages was investigated.
Methods: The purpose of this study was to investigate the structural characteristics of the fuel cell on its performance. The results show that the pressure and temperature in the catalyst layer (CL) of the cathode side are greater than the anode, and the temperature in the central regions of the catalyst layer is higher than the lateral regions. Also, the channel with a length of 100 mm is optimal in terms of producing the maximum current density and the amount of pressure drop is much lower than the channel with a length of 150 mm, which reduces the power consumption of the cell.

* Corresponding author.
** Corresponding author.
E-mail address: shadi.esmaili@iaukhsh.ac.ir (Sh. Esmaeili).

https://doi.org/10.1016/j.csite.2024.104760
Received 22 January 2024; Received in revised form 5 June 2024; Accepted 25 June 2024
Available online 27 June 2024

Significant findings: In general, a higher electric current is produced by increasing the thickness of the gas diffusion layer (GDL) and the catalyst layer. At a voltage of 0.8 V, with increasing thickness from 0.25 mm to 0.5 mm, the current density increases above 6 %. The percentage increase in current density at 60 °C–80 °C for 0.85 V and 0.75 V voltages is 42.1 % and 9.28 %, respectively.

Nomenclature

$\dot{G}^{Cr}$	the molar flux of water production in direct reaction
h_{evap}	latent enthalpy of evaporation [kJ.mol^{-1}]
h_{react}	enthalpy of water formation [kJ.mol^{-1}]
C_p	specific heat capacity [J.kg^{-1}.K^{-1}]
D_k^{eff}	diffusion coefficient [m^{2}s^{-1}]
V^{act}	activation voltage [V]
f_b	volumetric force [N.m^{-3}]
k_{eff}	thermal conductivity [W.m^{-1}.K^{-1}]
$\vec{u}$	velocity vector [m.s^{-1}]
c_k	mass fraction
F	Faraday constant [J.mol^{-1}.V^{-1}.K^{-1}]
h_{cl}	height of the catalyst layer [m]
I	current [A]
i	current density [A.m^{-2}]
j	density of the transfer current [A.m^{-2}]
M	molecular weight [g.mol^{-1}]
T	temperature [K]
V	voltage [V]
S	source term

Greek symbols

α	charge coefficient
σ	specific surface resistance [Ω.m^{-2}]
ε	porosity
μ	viscosity [Pa.s^n]
ρ	density [kg.m^{-3}]

Abbreviations

a	anode
c	cathode
CL	catalyst layer
GDL	gas diffusion layer
PEM	proton exchange membrane
ref	reference
DR	direct reaction
act	activation
evap	evaporation
rev	reversible

1. Introduction

Recently, many researchers have investigated ways to enhance heat transfer using different ways [1–3]. Due to growing concerns about declining oil resources and climate change, fuel cell technology has received a great deal of attention in recent years due to its high efficiency and low greenhouse gas emissions. Fuel cells, which are classified according to the electrolyte used in them, are electrochemical devices that directly convert the chemical energy stored in fuels such as hydrogen into electrical energy. Their efficiency can reach a significant amount of 60 % in the conversion of electrical energy and a total of 80 % in the simultaneous production of electricity and heat with more than 90 % reduction of major pollutants. The two most common types of fuel cells are proton exchange membrane fuel cells (PEMFCs) and solid oxide fuel cells (SOFCs). Due to the solid electrolyte of the PEM fuel cell and its flexibility, the possibility of breaking or cracking is low. Compared to other types of fuel cells, PEM fuel cells produce more power for a given volume and weight. This type of fuel cell requires little time to start due to low temperature, and this feature makes them the best option for in-vehicle applications as an alternative to diesel and gasoline internal combustion engines (as an example is examined in this

study). These systems are also suitable for use in home generators, small power plants, transportation and military industries. Fuel cell applications range from low-power [4] to high-power systems [5–7]. Fuel cells are powered by hydrogen and therefore must be equipped with a hydrogen production system [8,9]. Increasing performance and improving water and thermal management are some of the challenging problems in the PEM fuel cells [10–12]. Numerical analyses in the fuel cell can include a complete study of the fuel cell system [13], the study of bipolar plates [14], the study of the gas diffusion layer [15], the study of the catalyst layer [16] and the oxygen production system [17]. Sun et al. [18] investigated a 3-D, steady, and single-phase flow of a PEM fuel cell with a helical configuration. They studied pressure distribution and flow through the GDL. The gas flow channel with a trapezoidal cross-section was introduced in their study. The results showed that the aspect ratio of the trapezoidal cross-section (ratio of large base to small base) has a significant effect on the flow rate. As this ratio increases, the throughput flow through the GDL increases. This ratio also has a large effect on the change in field pressure. Ahmed and Song [19] simulated a PEM fuel cell with a three-dimensional, non-isothermal and raised membrane electrode assembly. In their study, the adjacent shoulders had different heights. The effect of variation of membrane electrode assembly on cell performance was investigated by maintaining the same reaction area and boundary conditions at high current densities. They found that the cathode voltage drop decreases significantly with increasing swelling of the membrane electrode set so that the reactants are more evenly distributed on the reaction surface. X. D. Wang et al. [20] numerically investigated the effect of cathode channel shape on transmission features and performance of a PEM fuel cell in a 3-D model and two-phase flow. They found that at high operating voltages, cells with various channel configurations performed similarly. Atyabi and Afshari [21] introduced a numerical model that provided a complete understanding of the basic principles of transfer phenomena in the fuel cell of a polymer membrane with a honeycomb flow field. The results showed that increasing the operating pressure leads to more oxygen distribution in the cathode electrode and increasing the permeability of the gas diffusion layer increases the uniformity of oxygen distribution and consequently the current density. Atyabi et al. [22] by placing one or more barriers in the cathode channel of the polymer membrane fuel cell, studied the dynamic effects of fluids due to the presence/absence of barriers in the channel as well as the barrier effect on fuel cell performance. Their results show that by placing a rectangular barrier, compared to the unobstructed state, the greatest increase in velocity occurs in the gas diffusion layer (below the barrier about 6 times the velocity) and more reactive gases are forced to enter. It was applied to the gas diffusion layer, which aided in chemical reactions and improved the fuel cell performance. They found that increasing the number of barriers also contributed to the transfer of reactive gases and the more uniform distribution of gases in the gas diffusion layer and the catalyst layer, especially at high current densities. Ghanbarian and Kermani [23] studied a proton exchange membrane fuel cell considering the single-phase flow of the reactant-product mixture at the air cell side electrode. The results show that channel indentation can increase the oxygen concentration content at the surface of the catalyst layer by up to 18 %. In 2015, Vazifehshenas et al. [24] numerically investigated the effects of the flow field on improving the performance of a PEM fuel cell. They showed that changing the flow field design could still be used as a practical way to improve performance. Rajabian et al. [25] designed and built a PEM fuel cell with a new flow channel pattern, called the symmetrical (new) spiral channel pattern. The battery had a rated power of about 10 W, an active area of 25 cm^2 and a Nafion-117 membrane. Using the fuel cell tester, the effect of temperature and relative humidity of the cathode gases on its performance (polarization curve) was investigated. Experimental results showed that the fabricated cell was able to produce a maximum power density (about 0.45 W/cm^2). Then, three-dimensional and complete numerical modeling of the built-in fuel cell (including all 9 layers of the fuel cell) was performed in real dimensions. The results of numerical modeling showed that the symmetric (new) helical channel can create the desired temperature distribution and concentration throughout the active region even at high current densities. Monsef et al. [26] investigated the effects of channel width, the number of coil channels, and flow direction on the consumption of reactants in a PEM fuel cell with cochlear flow field design numerically using FVM in cylindrical coordinates. Their findings show that the ratio of channel width to rib influences cell performance. The larger the ratio, the more important the contact area between the channel and the GDL, the more reactants penetrate the GDL, and the more uniform the distribution of reactants. Rostami et al. [27] studied a 3-D to understand the influence of bending size on a PEM fuel cells. The findings show that increasing the bend from 1 mm to 1.2 mm, not only significantly reduces the overvoltage, but also reduces the temperature gradient. A review of research on flow simulation in PEM fuel cells with different channel shapes shows that the common denominator of all this research is that most of them focus only on the cathode side of the PEM fuel cell and the different cross-sections. This is logical because the PEM fuel cell cathode is a water-producing electrode and is where flooding is most likely to occur. Sun et al. [28] studied channel-to-channel flow in a PEM-fuel-cell using a serpentine channel with a trapezoidal cross-sectional shape. Their results show that for both modes the pressure drop is significant but for cross-flow, the pressure drop tends to decrease across the channel. Perng and Wu [29] studied the trapezoid baffles effect on cell net power in a PEMFC. Their results showed that the maximum increase in cellular network power is 90 % with baffles with an angle of 60° and a height of 1.125 mm. Freire et al. [30] studied the operational parameters on the performance of PEMFCs having different (rectangular and trapezoidal) cross-section shape. Their results showed that the trapezoidal channel has a high ability to remove water from the cathode. However, recent experimental studies show that for certain operating conditions, overflow can occur in the anode gas channels and can be even more noticeable than on the cathode side [31–33]. A literature review shows that robust studies have been performed in relation to fuel cell simulations. However, most studies focus on the study of physical parameters (relative humidity, cell voltage, stoichiometric ratio, mass flow rate, etc.) and their impact on fuel cell performance. Also, in some studies, water and thermal management in fuel cells or flow channel design have been studied. Because one of the factors influencing the performance of the fuel cell is its configuration and structure, the need for a structural study was felt. Therefore, based on the literature review, it is observed that the effect of structural and physical properties on the fuel cell performance with a trapezoidal channel has not been studied so far.

1.1. Problem statement

Without considering the electrochemical equations of the cell, it is not possible to accurately study the performance of the cell. Consideration of other parts of the PEMFC (GDLs, CLs, BPs, and membrane) is necessary to investigate the phenomena involved in cell function, and such simulation is only possible with an integrated view of the cell. Therefore, in the present study, the effect of current channel cross-section geometry in both anode and cathode channels along with simulation of other parts of the cell on the performance of PEM fuel cell in the three-dimensional and permanent state is investigated and compared with conventional rectangular geometry. The geometry under consideration is shown in Fig. 1. As can be seen, the trapezoidal geometry is maintained in both the cathode and anode channels of the cell function. The properties of the materials used in the polymer fuel cell are presented in Table 1. The purpose of this study is to investigate the following.

- The effect of the cross-sectional shape of the anode and cathode channels on the performance of the PEM type fuel cell.
- The effect of temperature on the performance.
- The effect of GDL thickness on the performance.
- The effect of catalyst layer thickness on the performance of PEM fuel cell.

2. Mathematical description

2.1. Assumptions

The assumptions that are considered for the equations are as follows.

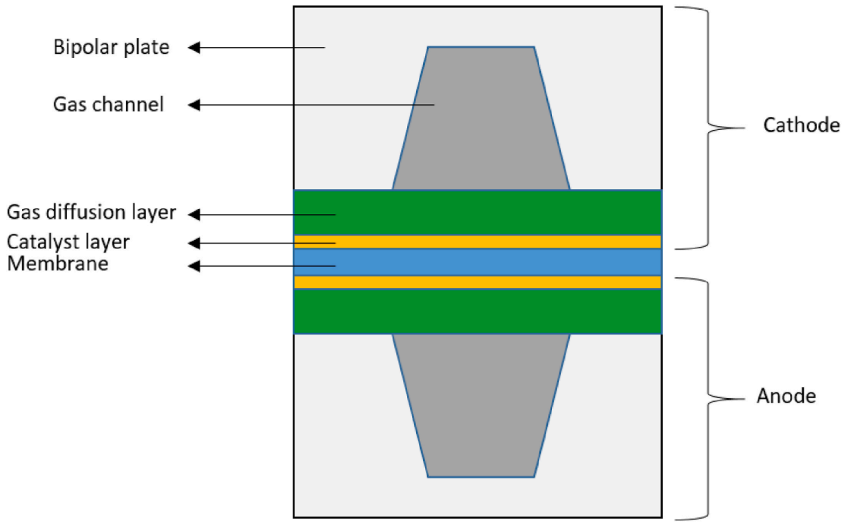

Fig. 1. Schematic of the problem.

Table 1
Parameters required simulating the PEM fuel cell.

Value	Unit	Characteristic	Component
7500	S/m	Electrical conductivity	Bipolar plate
31.5	W/m.K	Thermal conductivity	
4.5e+6	m^{-1}	Active level per unit volume	CL
1800	S/m	Electrical conductivity	
1.45e-11	M2	Permeability	
12	W/m.K	Thermal conductivity	
0.4	–	Porosity	
1800	S/m	Electrical conductivity	GDL
1.45e-11	M2	Permeability	
12	W/m.K	Thermal conductivity	
0.4	–	Porosity	
2719	kg/m^3	Density	
11000	kg/kmol	Equivalent weight	Membrane
0.36	W/m.K	Thermal conductivity	
1e-16	S/m	Electrical conductivity	
1980	kg/m^3	Density	

- The fluid flow inside the fuel cell channel is assumed to be steady (a common assumption in PEMFCs is due to the lack of phase change modeling).
- The flow is considered incompressible and laminar (the low pressure and velocity gradients justify this assumption).
- The behavior of the gases follows the ideal gas law (qualitatively, at different temperatures and pressures, many gases, such as hydrogen and oxygen, behave like an ideal gas in which molecules play the role of ideal particles).
- The relative humidity is considered to be 100 % for both the cathode and the anode (fuel cell performance is higher if the intake gases are completely humid).
- The effect of gravity is ignored (the convective and viscosity forces are much larger than the weight forces).
- The porous media in the cell are assumed to be homogeneous and isotropic (a realistic assumption in fuel cells, because there is uniformity of matter structure in every direction)
- Darcy's law is used to simulate a porous medium (because Darcy's law, in combination with laminar flow, has good accuracy).
- The flow is considered as a single-phase (using this assumption significantly reduces the complexity of the simulation and makes it easier to understand the physics of the problem).
- The membrane is impermeable to gases (if the membrane is permeable to the penetration of gases, the PEM fuel cell will malfunction).

2.2. Governing equations

The continuity equation is generally as follows [34],

$$\begin{cases} \varepsilon \nabla .\left(\rho \vec{u}\right) = S_m \\ S_m = 0 \end{cases} \Rightarrow \nabla .\left(\rho \vec{u}\right) = 0 \tag{1}$$

In Eq. (1), S_m represents the mass source, ρ represents the density, ε represents the porosity in the gas diffusion layer and the catalyst layer, and u represents the velocity. The fluid flow in the gas diffusion layer and the catalyst layer is in a porous medium, and there is a mass source in it because the chemical reaction of the fuel cell, which leads to the production of water and oxygen consumption, takes place inside the catalyst layer. In practice, the amounts of water production and oxygen consumption in different areas of the catalyst layer is not constant and have a direct relationship with the amount of current density produced in the catalyst layer, which is obtained from the Faraday relation. Since the channel is not a porous medium and there is no mass source in it, the continuity equation in the channel area is simpler (although the gas diffusion layer is a porous medium, there is no mass source in that area because no chemical reaction occurs).

The momentum equation is generally in the form expressed as follows [35],

$$\nabla .\left(\rho \varepsilon \vec{u}\vec{u}\right) = -\varepsilon \nabla P + \nabla .\left(\varepsilon \mu^{eff} \nabla \vec{u}\right) + f_b + S_u \tag{2}$$

In Eq. (2), S_u represents source term, P represents pressure, μ^{eff} represents effective viscosity, and f_b represents volumetric force. Considering the continuity equation and the momentum equation, at the inlet of the gas channels, the boundary condition of the mass flow rate is used. At the outlet of gas channels, the pressure outlet is used. The interior boundary condition is used to communicate with the internal parts of the fuel cell. For initial conditions, the temperature is assumed to be 353 K and the gauge pressure to be 0 Pa.

The \ equation of chemical components is generally expressed as follows [36],

$$\nabla .\left(\varepsilon \vec{u} c_k\right) = \nabla .\left(D_k^{eff} \nabla c_k\right) + S_k \tag{3}$$

In Eq. (3), S_k represents the source term, c_k represents the mass fraction, and D_k^{eff} represents the diffusion coefficient. In general, the index k represents the kth component of the chemical reaction. The Faraday equation in the catalyst layer of the PEM fuel cell is expressed as follows,

$$\dot{n}_{O_2} = -\frac{I}{4F}, \dot{n}_{H_2O} = \frac{I}{2F} \tag{4}$$

In Eq. (4), F shows the Faraday constant, I indicates the generated electric current in the catalyst layer, and $\dot{n}$ represents the number of moles of oxygen and water. In the catalyst layer, there is the expression for the source of the components, the value of which can be obtained according to the Faraday constant and the electric current produced. Therefore, it can be written as follows,

$$\begin{cases} \dot{n}_{O_2} = -\frac{I}{4F}, I = i \times A_{effective}, \dot{m}_{O_2} = M_{O_2} \dot{n}_{O_2} \\ S_{O_2} = -\frac{\dot{m}_{O_2}}{V_{cl}}, V_{cl} = A_{effective} \times h_{cl} \end{cases} \Rightarrow S_{O_2} = -\frac{M_{O_2} i}{4F \times h_{cl}} \tag{5}$$

Eq. (5) expresses the relationship between the oxygen consumption in the cathode electrode and the generated current density. A negative sign indicates oxygen consumption in the catalyst layer. M_{O_2} represents the mass of a mole of oxygen, h_{cl} indicates the height of the catalyst layer, and i represents the output current density. If, like oxygen for water, the necessary simplifications are made, the

relationship between water production at the cathode side and the current density generated in the catalyst layer results from Eq. (6). It should be noted that the positive sign indicates the water production in the catalyst layer.

$$S_{H_2O} = \frac{M_{H_2O} i}{2F \times h_{cl}} \tag{6}$$

The energy equation is generally for the porous medium in the form of Eq. (7). Each component of the phrase related to the energy source is shown in Eq. (8) [37,38],

$$\nabla.\left(\varepsilon \rho C_p \vec{u} T\right) = \nabla\left(k_{eff}.\nabla T\right) + Sp^{energy} \tag{7}$$

$$Su^{energy} = Su^0 + Su^{act} + Su^{DR} + Su^{evap} \tag{8}$$

In Eq. (8), Su^0, Su^{act},Su^{DR} and Su^{evap},respectively, represent heat generation due to the ohmic losses, reaction activation, direct reaction and evaporation of water. Each of the values of the heat generation in Eq. (8) can be determined from Eqs. (9a) to (9d),

$$Su^0 = i^2/\sigma \tag{9a}$$

$$Su^{DR} = \dot{G}^{Cr}.h_{react} \tag{9b}$$

$$Su^{act} = V^{act} j \tag{9c}$$

$$Su^{evap} = \dot{G}^{evap}.h_{evap} \tag{9d}$$

where j represents the density of the transfer current, indicates the rate at which a chemical reaction is carried out and includes the amount of material produced and consumed, the production of ions, and the release of electrons. V^{act} represents the activation voltage, $\dot{G}^{Cr}$ represents the molar flux of water production in direct reaction, h_{react} and h_{evap} represent the enthalpy of water formation at local temperature and the latent enthalpy of evaporation, respectively. Protons flow only in the catalyst layer and membrane, and i is zero in GDL. Activation and direct reaction terms are also zero except in the case of catalyst layers. Transmission enthalpy due to species distribution is neglected due to its small value. The charge equation is in the form of Eq. (10), and the source term due to the production of electric charge in the catalyst is expressed as follows [39],

$$\nabla(\sigma \nabla \Phi) = Su^{\Phi} \tag{10}$$

$$Su^{\Phi} = \begin{cases} +j & Anode\ catalyst \\ -j & Cathode\ catalyst \\ 0 & other\ location \end{cases} \tag{11}$$

The Butler-Volmer equation expresses the relationship between the operating voltage and the current density of the fuel cell so that according to the physical characteristics and operating conditions, the amount of operating voltage at any current density can be determined. The Butler-Volmer equation is expressed as follows [40],

$$V_{cell} = V_{rev} - \frac{RT}{\alpha_c F} \ln\left(\frac{i \Big/ C_g^{O_2}}{i_0 \Big/ C_{ref}^{O_2}}\right) - \sigma i \tag{12}$$

In Eq. (12), V_{cell} represents the operating voltage, V_{rev} represents the reversible voltage, α_c represents the cathode charge coefficient, and i_0 is the current density after which the voltage drop starts and its value is constant. $C_{ref}^{O_2}$ represents the oxygen concentration in standard conditions (temperature of 25 °C and pressure of 1 atm), $C_g^{O_2}$ represents oxygen concentration in fuel cell operating conditions. Also, σ represents the specific surface resistance. Since in the fuel cell, an electric current is generated in the catalyst layer, the Butler-Volmer equation is established in this region and the generated current is zero in the GDL and inside the channels. The values of the boundary conditions for the polymer fuel cell are presented in Table 2.

2.3. Grid study and validation

Since the different parts of the studied geometries are cubic and trapezoidal, rectangular and trapezoidal grids were selected to mesh the geometry. For different areas of the solution range, meshes with different sizes are considered. For example, since electrochemical reactions take place in the catalyst layer and its thickness is very small, we should have smaller meshes than the parts related to the gas passage channel. To investigate the grid independency, models with different numbers of cells were created and their results were compared with each other. First, the number of cells was less and then, step by step, we increase the number of cells in different parts until the number of cells did not change much in the obtained answers. It is clear that in this case, to reduce the computation time, the minimum number of cells should be used, after which the results are not changed. Fig. 2 shows the meshing of the gas channels with a trapezoidal channel, and Fig. 3 shows the meshing of the channel with the GDL and the CL. As described, it can be

Table 2
Boundary conditions in the present work.

Value	Unit	Boundary condition	
70	˚C	Fuel cell temperature	
70	˚C	Humid anode temperature	
70	˚C	Humid cathode temperature	
3	atm	Anode reverse pressure	
3	atm	Cathode reverse pressure	
4.9e-8	kg/s	Anode flow rate	
6.82e-7	kg/s	Cathode flow rate	
1.1	V	Open circuit voltage	
49.5	%	H_2	Anode inlet mass fraction
50.5	%	H_2O	
21.8	%	O_2	Cathode inlet mass fraction
6.6	%	H_2O	
71.6	%	N_2	

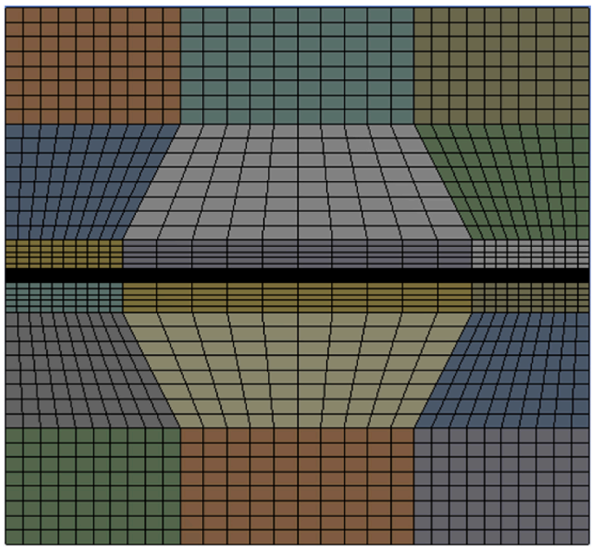

Fig. 2. Meshing of gas channels from a longitudinal section.

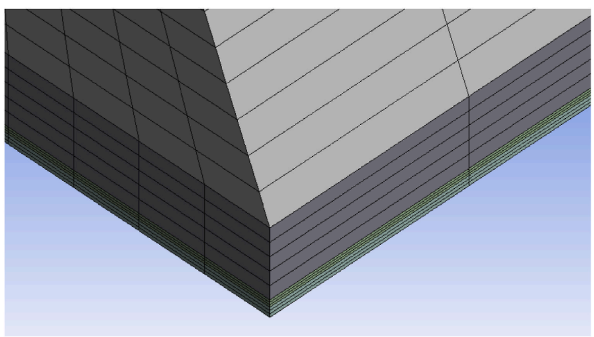

Fig. 3. Channel mesh with gas diffusion layer and catalyst layer.

seen that the mesh size of the catalyst layer is much smaller than the mesh along the longitudinal axis of the channel. Fig. 4 also shows a three-dimensional image of the model in ANSYS FLUENT 2020 R2. To check the appropriate number of meshes in the z-direction, which is in the direction of the channel length, the first 30 meshes were considered, but in each step by increasing the number of meshes in the longitudinal direction of the channel (50 meshes), the 93000 meshes were obtained. Table 3 shows the results of grid independency. Table 3 shows the results of the grid independency for the trapezoidal channel of the anode and cathode, according to which in the case of 93000, the number of cells has reached the correct solution value and this number of cells is sufficient. In cases with less mesh number, the number of required repetitions to converge the answer is very high and even in some intervals, the oscil-

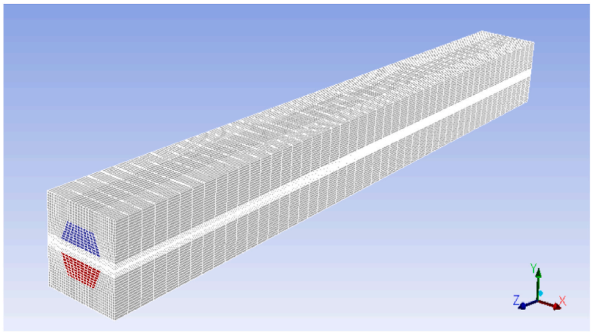

Fig. 4. Three-dimensional view of the meshed geometry.

Table 3
Results of grid independency at 0.5 V.

130200	93000	67700	19000	Mesh
1.3961	1.3956	1.3926	1.3908	Current density ($A.m^{-2}$)

lating answer is observed. One hundredth is the same, but at 93,000 cells, both the convergence rate and the accuracy of the answer are acceptable, and there is no need to make the meshes smaller.

When solving a problem numerically, it is necessary to compare the numerical results with the experimental results obtained by others. Even when the analytical solution or experimental measurement is performed, comparing the obtained results with the results of previous works is very useful and the accuracy of the research is correct. Although many experimental and numerical studies are done in the field of polymer fuel cells, there are not many comprehensive experimental studies. One of the most comprehensive experimental studies in this field was conducted by L. Wang et al. [41], which was the reference for many experimental and numerical studies to validate their results. A model similar to Wang's model is simulated and its results are compared with the experimental results in this paper. The cell is checked stably and isothermally (at 70 °C) and the flow at the anode and cathode is considered to be in the opposite direction. The dimensions of the polymer membrane fuel cell related to L. Wang et al. [41] are shown in Table 4. Here, to validate the results, at different voltages, the simulation results are compared with the experimental results obtained in the paper, which are shown in Table 5. In another study, Yan et al. [42] experimentally considered the steady-state performance of a PEM fuel cell. In addition to the polarization curve, they examined the effects of temperature, relative humidity, and pressure on current density and power density. In their work, the studied fuel cells had an area of 5 cm^2–25 cm^2. The active membrane area was assumed to be 49 cm^2 and the fuel cell performance was tested at pressures of 1–4 atm, relative humidity of 0 %–100 % up to 85 °C. Fig. 5 shows the changes in current density with cell voltage at 100 % relative humidity. As can be seen, an acceptable correlation is seen between the present work and the experimental reference [42].

Table 4
Dimensions of fuel cell (L. Wang et al. [41]).

Thickness (mm)	Component
0.051	Membrane
0.26	GDL
0.0129	CL
70	Channel length
1	Channel height
0.9	Channel weight
1.5	Bipolar plate height
1.8	Bipolar plate weight

Table 5
Comparison of the present work and Ref. [41].

Current density ($A.m^{-2}$)		
Present work	L. Wang et al. [41]	Voltage (V)
0.0317	0.0316	0.9
0.3228	0.3118	0.8
0.8189	0.8831	0.7
1.2411	1.1241	0.65
1.3459	1.2338	0.6

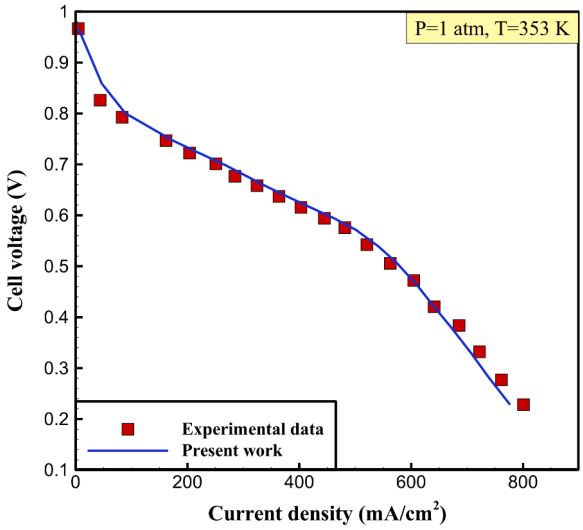

Fig. 5. Comparison of the present work with experimental data [42].

3. Results

3.1. Investigation of the effect of anode and cathode channel cross-sectional shape on PEM fuel cell performance

One of the most important parameters to determine the geometry of the fuel cell channel is to determine the appropriate length for it. To obtain the appropriate length, various criteria should be considered, such as increasing the density of the production current from the cell and limiting the space for using the fuel cell.

3.1.1. Influence of channel developing length on cell performance

In this simulation, four different lengths of 50, 25, 100, and 150 mm are considered for the channel length. Taking into account the operating conditions mentioned in the previous sections, a working voltage of 0.8 V was imposed for all three simulation modes. The results obtained from channel simulations with different lengths are shown in Fig. 6. According to the results obtained from this figure, by increasing the length of the channel from 25 to 150 mm, the generated electric current increases.

According to the results obtained from the contours shown in Fig. 7a to d, it can be said that at lengths of 25 and 50 mm, the flow is not yet developed, but at 100 flows it reaches a fully developed. If the channel length is appropriate, the reactants have their maximum value at the input and after the reaction along the channel, they are consumed due to the reaction and at the output, their molar fraction decreases and they leave the channel at a minimum value. In this case, an electric current is generated from most of the active surface of the cell, which leads to improved cell performance. In addition, using the appropriate channel length becomes more important in situations where there is limited space to use the fuel cell. Therefore, if the only selection criterion is the generated electric cur-

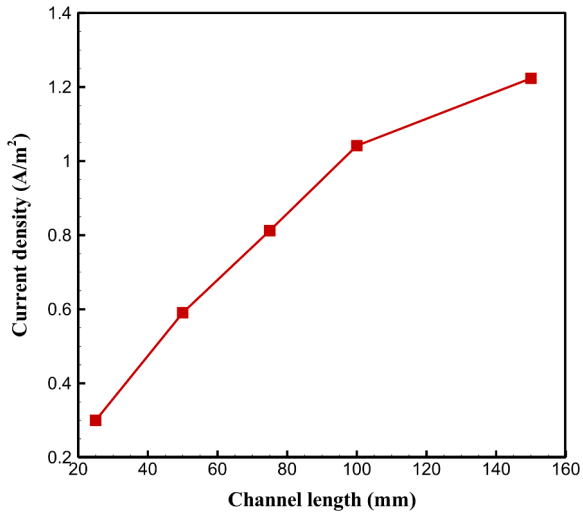

Fig. 6. Results of channel simulation with different lengths (V = 0.8 V).

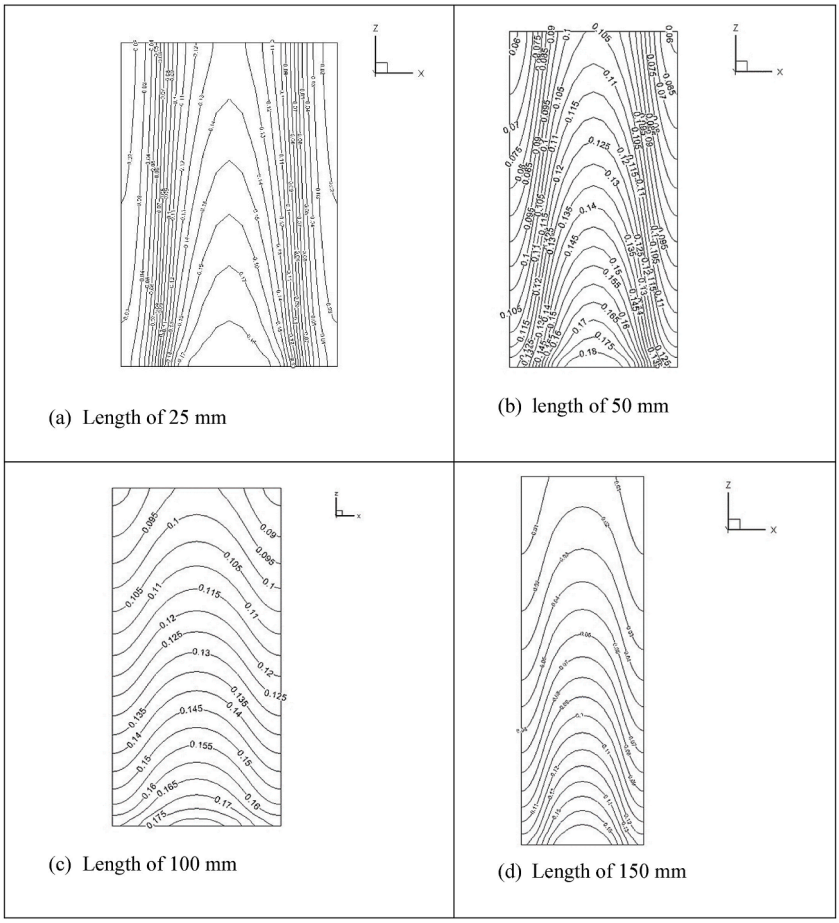

Fig. 7. Contour of oxygen mole fraction in the middle of the cathode side catalyst layer.

rent, the selected length for the next steps is 150 mm, while in addition to other parameters such as the active surface of the cell, the power consumption required to create fluid flow inside the channel and space constraints must be considered.

The active surface of the cell with different dimensions is shown in Fig. 8. In this figure, L represents the length of the channel and W represents the width of the channel, and their product is equal to the active surface of the fuel cell. For the comparison between different lengths to be the same, the amount of fuel cell-active surface for the channel with different lengths must be kept constant. The following conditions must be met to keep the activity level constant,

$$A = L_1 W_1 = L_2 W_2 \tag{13}$$

Considering these conditions, the obtained results for different lengths are shown in Fig. 9. According to the obtained results, the channel with a length of 100 mm is optimal because the density of the output current is the maximum, which increases the production capacity of the cell. Also, the amount of pressure drop is much less than when the channel length is 150 mm, which reduces the

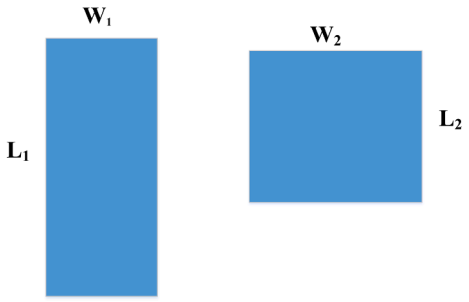

Fig. 8. Active cell surface with different dimensions.

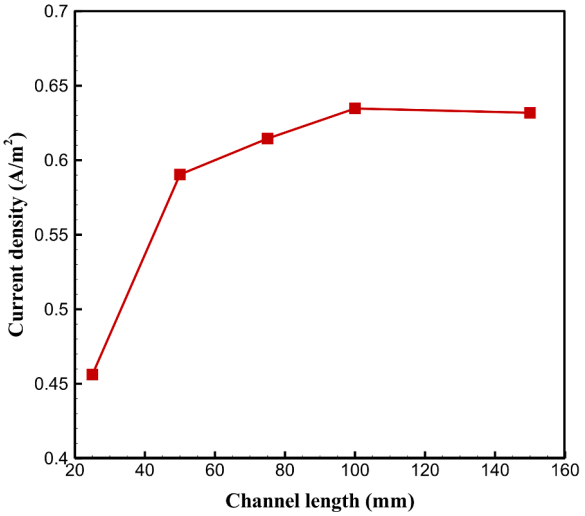

Fig. 9. Simulation results with different lengths and fixed active surface (V = 0.8 V).

amount of power consumption of the cell. In addition, for places where space is limited, a length of 150 is preferable to a cell. The molar fraction of oxygen in the middle of the catalyst layer on the cathode side for a 25 mm long channel is shown in Fig. 7a. In this case, the reactants leave the channel before they react enough and are consumed to increase the density of the output current, which reduces the performance of the fuel cell. The molar fraction of oxygen in the middle of the catalyst layer on the cathode side is shown in Fig. 7b for a 50 mm long channel. In this case, the reactants are consumed after the reaction along the channel, due to the reaction, and at the output, the amount of their molar fraction is reduced and they leave the channel. The molar fraction of the reactants, even near the output, is such that if the channel length was longer and more of them were consumed during the reaction, it would still be possible to react and generate electricity at the output, so the channel length would be less than its optimal length. The molar fraction of oxygen in the middle of the catalyst layer on the cathode side is shown in Fig. 7c for a 100 mm long channel. In this case, the reactants are consumed after the reaction along the channel, due to the reaction, and at the output, the amount of their molar fraction is reduced and they leave the channel. The molar fraction of the reactants, even near the outlet, is such that an electric current is generated from most of the cell's active surface, which improves the cell's performance. In addition, using the appropriate channel length becomes more important in situations where there is limited space to use the fuel cell. The molar fraction of oxygen in the middle of the catalyst layer on the cathode side is shown in Fig. 7d for a channel with a length of 150 mm. According to the obtained results, the reactants in one length of the channel are completely consumed due to the reaction and their amount is so low that they can no longer react in the catalyst layer and there will be no production current density in these areas. The channel does not increase the amount of electric current produced and its ratio per unit area decreases, thus reducing the performance of the fuel cell. In addition, increasing the duct length is not recommended and is not recommended in situations where there is limited space to use the fuel cell, and as a result, it is undesirable in this regard. In addition to the above, the parameter of the amount of inlet pressure created to create a fluid flow inside the channel that is directly related to power consumption should be considered. In this case, only the lengths of 100 and 150 mm are compared because the amount of current density generated from them is close to each other, and to discuss the net power output, the amount of power consumption must be compared with each other. The amount of pressure gradient in the channel is important so that the reactants can travel the length of the channel and the reaction rate is higher. On the other hand, a high value of the pressure gradient increases the power consumption in the fuel cell, which is undesirable. As a result, the pressure drop parameter plays an important role in selecting the appropriate channel length.

The pressure contour in the middle of the catalyst side catalyst layer is shown in Fig. 10 for a 100 mm long channel. Since the outlet pressure is equal to the ambient pressure, the amount of pressure at the inlet is equal to the pressure created by the inlet air pump to the cell. Due to the symmetry of the channel geometry, the pressure contour is also symmetrical and the amount of pressure decreases uniformly from the inlet to the outlet.

The pressure contour in the middle of the catalyst layer on the cathode side is shown in Fig. 11 for a channel with a length of 150 mm. In this case, as in the previous case, the amount of pressure at the inlet is equal to the pressure created by the inlet air pump to the cell. The pressure contour is symmetrical and the amount of pressure from the inlet to the outlet decreases uniformly. According to the obtained results, the amount of pressure at the inlet of the channel with a length of 150 mm is about 3.5 times that of the channel with a length of 100 mm, which causes a drop in power consumption of about 3.5 times. Therefore, considering that the amount of generated current density from the channel with a length of 100 mm is higher and its pressure drop is less, a length of 100 mm is more suitable for the channel. In the discussion of the pressure parameter, the difference in the amount of pressure on the cathode and anode sides is investigated.

Figs. 12 and 13 show the pressure contour in the middle of the channel with a length of 150 mm and the pressure contour in the middle of the catalyst layer at the anode side, respectively. According to the obtained results, the amount of pressure at the input of

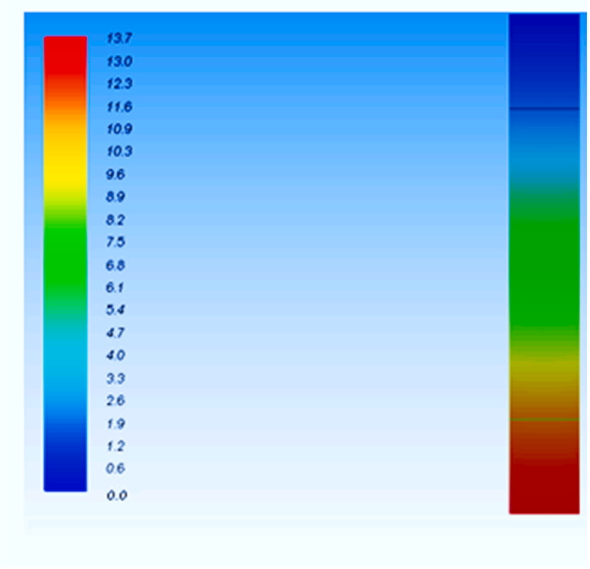

Fig. 10. The relative pressure contour (in terms of Pa) in the middle of the catalyst side catalyst layer for a channel with a length of 100 mm.

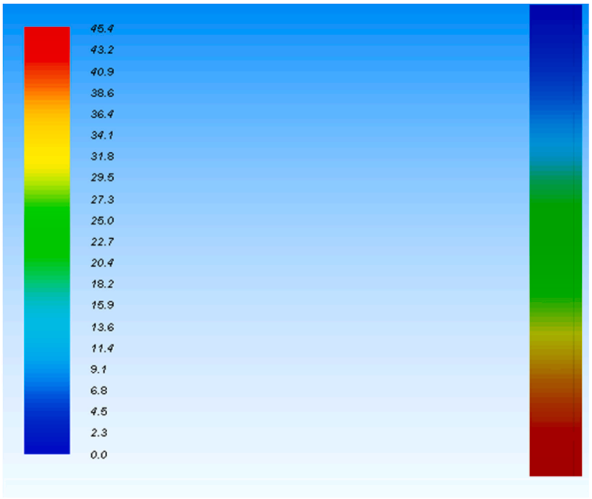

Fig. 11. The relative pressure contour (in terms of Pa) in the middle of the catalyst side catalyst layer for a channel with a length of 150 mm.

the anode side from the cathode side is less. In this case, as in the previous case for the cathode, the pressure contour is symmetrical and the amount of pressure decreases uniformly from the inlet to the outlet. It can be concluded from Fig. 13 that the flow velocity at the anode side is faster than the cathode. Therefore, more hydrogen is expected to be consumed.

3.1.2. Influence of channel dimensions on cell performance

To investigate the effect of geometry, in addition to the channel length, the trapezoidal sides of the cathode and anode channels have also been investigated. In changing the geometric dimensions of the channel, it has been noticed that in both cases, the hydraulic diameters of the two channels are equal to each other. If we denote the sides of the channel by a and b and the height of the channel by h, the value of the hydraulic diameter denoted by D_h can be obtained from the formula. In this formula, A is the area of the channel and P is the circumference of the channel, which is the height of the channel according to the amount and ratio of trapezoidal sides.

$$D_h = \frac{4A}{P} = \frac{2h\,(a+b)}{p} \tag{14}$$

Figs. 14 and 15 show the cross-sections of cathode and anode channels with two ratios of 1/3 and 2/3, respectively. By placing the values shown, the value of the hydraulic diameter for this geometry is 1.4 mm. In the second case, the ratio of the sides of the channel is as shown in Fig. 15. By equating the hydraulic diameter in the two shown cases, the height of the channel in the second case is 1.25 mm. After determining the new dimensions of the channel, the simulations were performed with the same operating

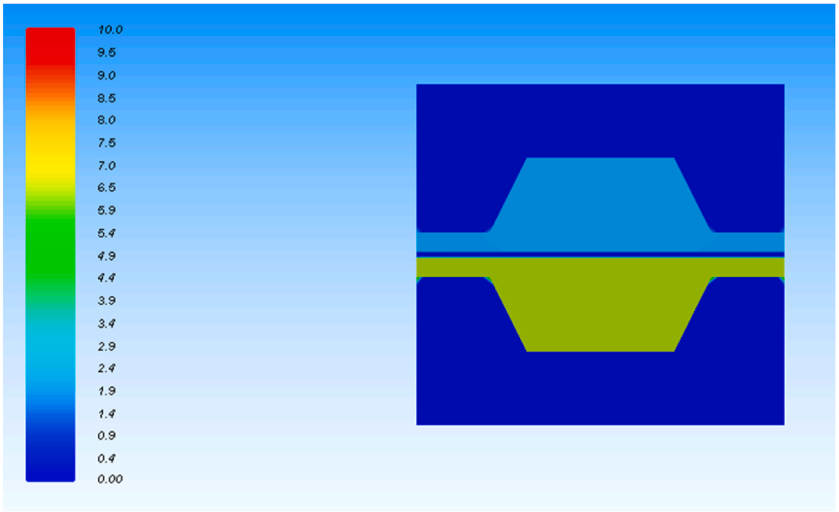

Fig. 12. Relative pressure contour (in terms of Pa) in the middle section of the channel with a length of 150 mm.

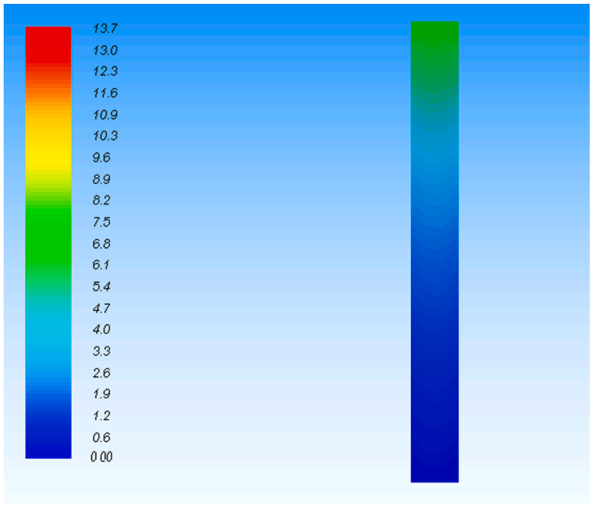

Fig. 13. The relative pressure contour (in terms of Pa) in the middle of the catalyst layer at the anode side for a channel with a length of 150 mm.

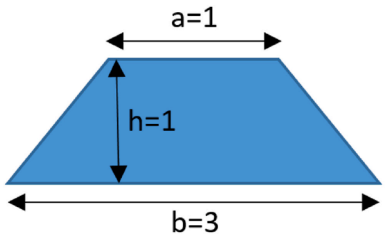

Fig. 14. Cross section of cathode and anode channels with ratio 1/3.

conditions, the results of which are shown in Table 6. According to the obtained results, in the case where the ratio of the sides is 2/3, the density of the generated electric current is higher, and as a result, these dimensions are considered for the channel at the anode and cathode side of the fuel cell.

3.1.3. Investigation of the effect of GDL thickness on PEM fuel cell performance

Another factor affecting the performance of the fuel cell is the thickness of the penetration layer of the fuel cell, which was studied in this section. As explained in the previous section, to determine the dimensions of the channel, in determining the thickness of the GDL, it should be noted that its thickness should not be increased as much as possible so that the space occupied by the cell is less and on the other hand the output current density is high. For the cell, three different modes of GDL with thicknesses of 0.25, 0.5 and

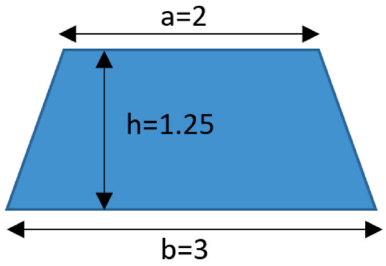

Fig. 15. Cross section of cathode and anode channels with ratio 2/3.

Table 6
Results of channel simulation with different sides (V = 0.8 V).

2/3	1/3	Ratio of channel sides
1.0413	1.0265	Current density ($A.m^{-2}$)

0.75 mm are considered. The results obtained for these three cases are shown in Fig. 16. According to the obtained results, by increasing the thickness of the GDL from 0.25 to 0.50 mm, the amount of production current density has increased, but when the thickness reached 0.50 mm–0.75 mm, the amount of production current density has remained constant. As a result, the appropriate thickness for the GDL is 0.50 mm because the production current density is higher than the 0.25 mm thickness and takes up less space than 0.75 mm.

3.1.4. Investigation of the effect of catalyst layer thickness on PEM fuel cell performance

Another factor affecting the performance of the fuel cell is the thickness of the catalyst layer of the cell, which is examined in this section. As explained in the previous section to determine the dimensions of the thickness of the gas penetration layer, in determining the thickness of the catalyst layer, it should be noted that its thickness should not be increased so that the space occupied by the fuel cell is less and on the other hand the current density is also high. For the cell, three different states of the catalyst layer with thicknesses of 0.25, 0.5 and 0.75 mm have been considered. The results obtained for these three cases are shown in Fig. 17. According to the obtained results, with increasing the thickness of the gas penetration layer from 0.25 to 0.50 mm, the amount of production current density has increased, but when the thickness has reached from 0.50 to 0.75 mm, the amount of production current density has remained constant. As a result, the appropriate thickness for the catalyst layer is 0.50 because the production current density is higher than the 0.25 mm thickness and takes up less space than 0.75 mm.

3.1.5. Investigation of the effect of temperature on the performance of PEM fuel cell

One of the most important operating conditions for a polymer membrane fuel cell is the operating temperature of the cell. In general, polymer membrane cells are considered as low-temperature types, therefore, to investigate the effect of temperature, functional temperatures should be considered in their operating range. For this purpose, the studied temperatures of 60, 70 and 80 °C were considered. Another noteworthy point in this regard is that according to the authoritative article and X. D. Wang et al. [20], which was

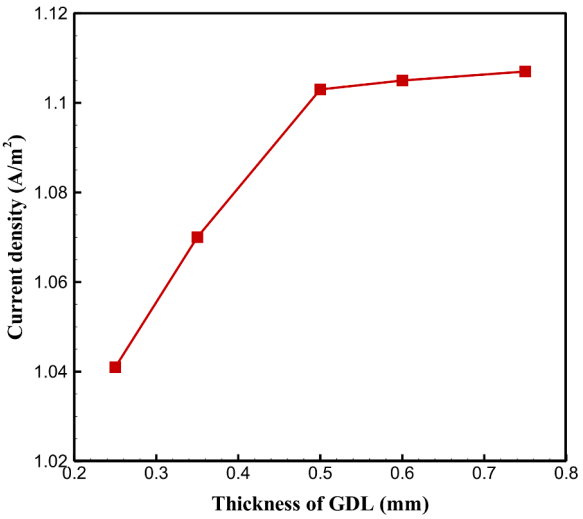

Fig. 16. Simulation results with different thicknesses of the GDL (V = 0.8 V).

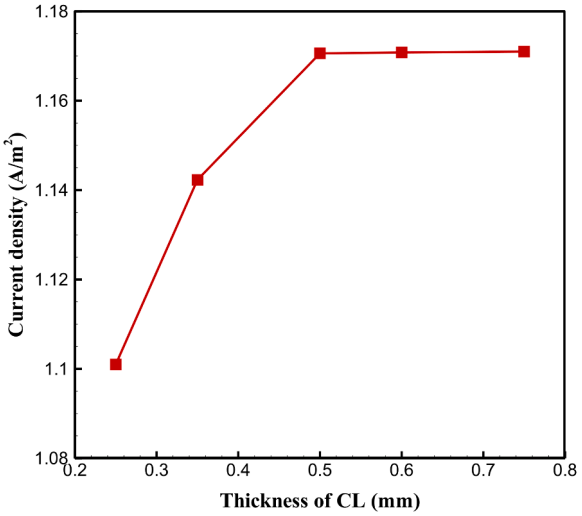

Fig. 17. Simulation results with different thicknesses of the CL (V = 0.8 V).

also used in the validation section, for the case that the working pressure of the cell is about 3 atm, the effect of temperature is different in two ways. At higher voltages, with increasing temperature, the amount of generated current density decreases and after a voltage of about 0.75 V, the effect is reversed, i.e. with increasing temperature; the amount of generated electric current density will be higher. In this part of the simulation, this has been considered. For this purpose, simulations have been performed at voltages of 0.85 V, 0.8 V and 0.75 V. The results obtained are shown in Fig. 18. According to the results obtained at a voltage of 0.85 V, with increasing temperature, the amount of electric current produced has increased, which is also significant. By reducing the operating voltage of the cell to 0.8 V, the amount of electric current produced has very little change with temperature. Once again, by reducing the operating voltage of the cell to 0.75, the trend of changes with temperature changes so that with increasing temperature, the amount of electric current produced increases. These results are consistent with the results obtained from X. D. Wang et al. [20].

Fig. 19 shows the temperature contour in the catalyst layer on the cathode side. The noteworthy point in the obtained results is that the amount of temperature in the middle areas of the catalyst layer is higher because in these areas the reaction rate is higher and the amount of heat exchange with the outside environment for cooling is also lower. Another conclusion that can be drawn from this figure is that by moving along the flow, the temperature decreases, which is also due to the reduction of the reaction rate at the channel output due to the presence of fewer reactants at the channel output. Given that the temperatures studied in this simulation were within the normal range of fuel cell performance, the amount of temperature increase in the middle regions of the catalyst layer is not a problem. If the operating temperature of the cell is higher, this increase in temperature can lead to a severe drop in cell performance and even membrane defects.

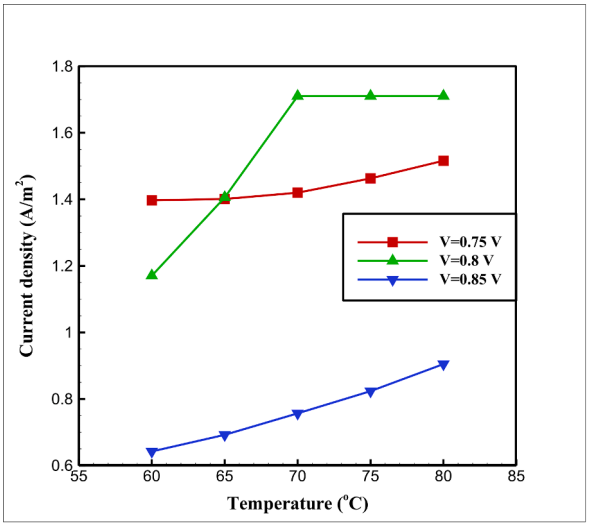

Fig. 18. Simulation results at different voltages and temperatures.

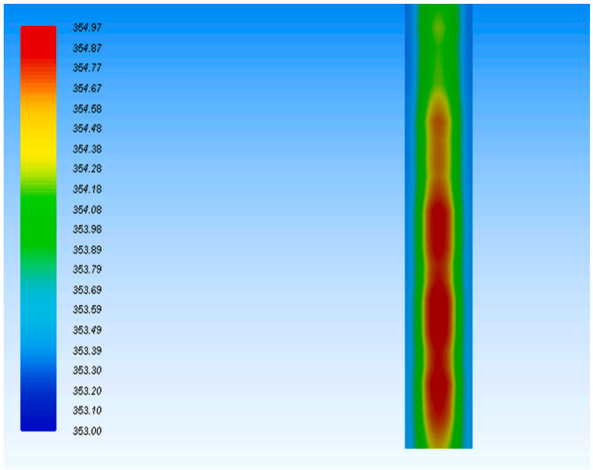

Fig. 19. Temperature contour (in terms of Kelvin) in the catalyst layer on the cathode side.

Fig. 20 shows the temperature contour in the catalyst layer at the anode side. As in the previous section, the temperature is higher in the central regions of the anode, and as it moves along the channel, the operating temperature of the cell decreases because the reaction rate is lower at the outlet of the channel. Comparing the shapes related to the cathode and anode temperature contour, it can be concluded that in general, the temperature value on the cathode side is higher than the anode and the reaction rate of the cathode side is higher than the anode. On the other hand, the cathode side may be exposed to more thermal stresses, so it is necessary to use a stronger cooling mechanism on the cathode side.

4. Discussion

In this study, a structural approach to fuel cell performance was investigated. The two most important components in a fuel cell are the gas diffusion layer and the catalyst layer, the thickness of which greatly affects the performance of the fuel cell. Most experimental studies focus on water and thermal management [43,44] and the improvement of the physical properties of these two components by considering their thickness [45,46]. On the other hand, most numerical studies examine the physical characteristics of fuel cell performance [47–50]. Therefore, numerical study by structural analysis of these two components considering the trapezoidal channel is a prominent feature of this research. This study follows a single-phase model using the finite volume method. Using a single-phase model makes it easier to understand the phenomena in the fuel cell and facilitates mathematical understanding of the equations. However, the two-phase model is more accurate and has a higher computational cost [51]. However, as a suggestion, it is recommended that researchers study thermodynamic irreversibility, new flow channel designs, energy analysis, and exergy, assuming a multiphase model.

5. Conclusion

In this research, the effect of anode and cathode channel cross-sectional shape on the performance of PEM fuel cell was investigated and the appropriate length and dimensions of the channel were determined. Finally, for the determined geometric conditions, the cell performance at different voltages was investigated. The purpose of this study was to investigate the structural characteristics

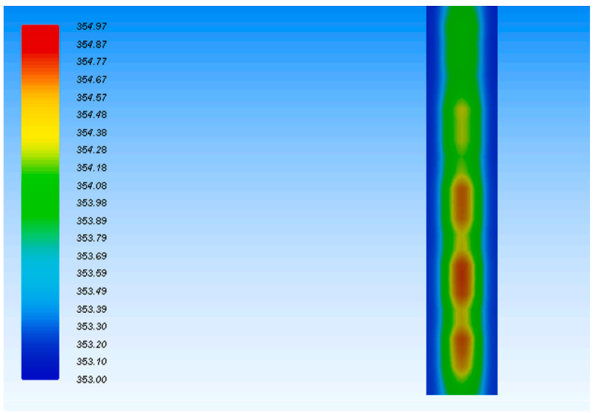

Fig. 20. Temperature contour (in terms of Kelvin) in the catalyst layer on the anode side.

of the fuel cell on its performance. Given that most studies had examined the physical characteristics of fuel cell performance, a structural study was needed. The summary of the results obtained from this research is as follows.

- The channel with a length of 100 mm is optimal because the density of the output current is the maximum, which increases the production capacity of the cell.
- As the thickness of the GDL increases, more electric current is generated.
- The appropriate thickness for the GDL is 0.50 mm.
- The appropriate thickness for the catalyst layer is 0.50 mm because the production current density is higher than the 0.25 mm thickness and takes up less space than 0.75 mm.
- At a voltage of 0.85 V, with increasing temperature, the amount of electric current produced increases, and this amount is also significant.
- By reducing the operating voltage of the cell to 0.8 V, the amount of electric current produced has very little change with temperature.

Suggestion

In line with the present study, the following suggestions are recommended for further studies.

- Investigation of multi-phase flow and comparison with single-phase flow considering irreversibility.
- Energy and exergy analysis of the PEM fuel cell with different gas channels.
- Water and thermal management in the PEM fuel cells with coolant channels.

CRediT authorship contribution statement

Sajad Hamedi: Supervision, Writing – review & editing; Conceptualization, Data curation, Formal analysis. **Ali Basem:** Investigation, Writing – original draft. **Murtadha M. Al-Zahiwat:** Formal analysis, Writing – original draft. **Ahmed Khudhair AL-Hamairy:** Investigation, Writing – original draft. **Dheyaa J. Jasim:** Supervision, Writing – review & editing. **Soheil Salahshour:** Writing – review & editing; Conceptualization, Data curation, Formal analysis. **Sh. Esmaeili:** Supervision, Writing – review & editing; Conceptualization

Declaration of competing interest

The authors declare that they have no known competing financial interests or personal relationships that could have appeared to influence the work reported in this paper.

Data availability

No data was used for the research described in the article.

References

[1] B. Jalili, N. Aghaee, P. Jalili, D. Domiri Ganji, Novel usage of the curved rectangular fin on the heat transfer of a double-pipe heat exchanger with a nanofluid, Case Stud. Therm. Eng. 35 (102086) (2022) 102086, https://doi.org/10.1016/j.csite.2022.102086.
[2] P. Jalili, K. Kazerani, B. Jalili, D.D. Ganji, Investigation of thermal analysis and pressure drop in non-continuous helical baffle with different helix angles and hybrid nano-particles, Case Stud. Therm. Eng. 36 (102209) (2022) 102209, https://doi.org/10.1016/j.csite.2022.102209.
[3] B. Jalili, P. Jalili, Numerical analysis of airflow turbulence intensity effect on liquid jet trajectory and breakup in two-phase cross flow, Alex. Eng. J. 68 (2023) 577–585, https://doi.org/10.1016/j.aej.2023.01.059.
[4] T. HenriquesB. CésarP, J. Costa Branco, Increasing the efficiency of a portable PEM fuel cell by altering the cathode channel geometry, A numerical and experimental study 87 (2010) 1400–1409.
[5] P. Sarmah, T.K. Gogoi, R. Das, Estimation of operating parameters of a SOFC integrated combined power cycle using differential evolution based inverse method, Appl. Therm. Eng. 119 (2017) 98–107.
[6] Y. Wang, B. Seo, B. Wang, N. Zamel, K. Jiao, X.C. Adroher, Fundamentals, materials, and machine learning of polymer electrolyte membrane fuel cell technology, Energy and AI 1 (100014) (2020) 100014, https://doi.org/10.1016/j.egyai.2020.100014.
[7] T.K. Gogoi, R. Das, A combined cycle plant with air and fuel recuperator for captive power application. Part 2: inverse analysis and parameter estimation, Energy Convers. Manag. 79 (2014) 778–789.
[8] P. Barnoon, D. Toghraie, B. Mehmandoust, M.A. Fazilati, S.A. Eftekhari, Comprehensive study on hydrogen production via propane steam reforming inside a reactor, Energy Rep. 7 (2021) 929–941.
[9] P. Barnoon, Modeling of a high temperature heat exchanger to supply hydrogen required by fuel cells through reforming process, Energy Rep. 7 (2021) 5685–5699.
[10] M. Rahimi- Esbo, A.A. Ranjbar, S.M. Rahgoshay, Analysis of water management in PEM fuel cell stack at dead-end mode using direct visualization, Renew. Energy 162 (2020) 212–221.
[11] P. Agus, S. SasmitoTariq ShamimArun, Mujumdar, Passive Thermal Management for PEM Fuel Cell Stack under Cold Weather Condition Using Phase Change Materials (PCM), 58, 2013, pp. 615–625.
[12] T. HenriquesB. CésarP, J. Costa Branco, Increasing the efficiency of a portable PEM fuel cell by altering the cathode channel geometry: a numerical and experimental study, Appl. Energy 87 (2010) 1400–1409.
[13] N. Ahsan, A Al Rashid, A.A. Zaid, Sikandar, R. Imran, Abdul Qadir, Performance analysis of hydrogen fuel cell with two-stage turbo compressor for automotive applications, Energy Rep. 7 (2021) 2635–2646.
[14] P. Barnoon, D. Toghraie, B. Mehmandoust, M.A. Fazilati, S.A. Eftekhari, Natural-forced cooling and Monte-Carlo multi-objective optimization of mechanical and thermal characteristics of a bipolar plate for use in a proton exchange membrane fuel cell, Energy Rep. 8 (2022) 2747–2761.
[15] B. Kumar, K. Pitambar, R. Sukumar Pati, Numerical investigation of multi-layered porosity in the gas diffusion layer on the performance of a PEM fuel cell, Int. J. Hydrogen Energy 45 (2020) 21836–21847.
[16] Y. Zhang, X. Li, A. Klinkova, Numerical investigation of delamination onset and propagation in catalyst layers of PEM fuel cells under hygrothermal cycles, Int. J.

Hydrogen Energy 46 (2021) 11071–11083.
[17] Y. Jia, M. Zeng, P. Barnoon, D. Toghraie, CFD simulation of time-dependent oxygen production in a manifold electrolyzer using a two-phase model, Int. Commun. Heat Mass Tran. 126 (2021) 105446.
[18] L. Sun, P.H. Oosthuizen, K.B. McAuley, A numerical study of channel-to-channel flow cross-over through the gas diffusion layer in a pem-fuel-cell flow system using a serpentine channel with a trapezoidal cross-sectional shape, Int. J. Therm. Sci. 45 (10) (2006) 1021–1026.
[19] D.H. Ahmed, H.J. Sung, Design of a deflected membrane electrode assembly for PEMFCs, Int. J. Heat Mass Tran. 51 (2008) 5443–5453.
[20] X.D. Wang, G. Lu, Y.Y. Duan, D.J. Lee, Numerical analysis on performance of polymer electrolyte membrane fuel cells with various cathode flow channel geometries, Int. J. Hydrogen Energy 37 (2012) 15778–15786.
[21] S.A. Atyabi, E. Afshari, Effect of GDL porosity and pressure on the PEM fuel cell performance with honeycomb flow-field, Journal of Solid and Fluid Mechanics 3 (3) (2013) 109–119.
[22] S.A. Atyabi, E. Afshari, M. Adami, Effects of baffle-blocked flow cathode channel on reactant transport and cell performance of a PEMFC, Modares Mechanical Engineering 14 (4) (2014) 158–166.
[23] A. Ghanbarian, M.J. Kermani, Performance improvement of PEM fuel cells using air channel indentation; Part I: mechanisms to enrich oxygen concentration in catalyst layer, Iranian Journal of Hydrogen & Fuel Cell 4 (2014) 199–207.
[24] Y. Vazifeshenas, K. Sedighi, M. Shakeri, Numerical investigation of a novel compound flow field for PEMFC performance improvement, Int. J. Hydrogen Energy 40 (2015) 15032–15039.
[25] H. Rajabian, H. Amiri, M. Rahimi, S.M.B. Marashi, A.A. Arab Solghar, Experimental and numerical analysis of PEM fuel cell performance with a new helically symmetrical flow channel, Journal of Solid and Fluid Mechanics 6 (4) (2016) 285–300.
[26] T. Monsaf, B.M. Hocine, S. Sahli Youcef, M. Abdallah, Unsteady three-dimensional numerical study of mass transfer in PEM fuel cell with spiral flow field, Int. J. Hydrogen Energy 42 (2017) 1237–1251.
[27] L. Rostami, P.M.G. Nejad, A. Vatani, A numerical investigation of serpentine flow channel with different bend sizes in polymer electrolyte membrane fuel cells, Energy 97 (2016) 400–410.
[28] Lan Sun Patrick H. OosthuizenKim B. McAuley, A numerical study of channel-to-channel flow cross-over through the gas diffusion layer in a PEM-fuel-cell flow system using a serpentine channel with a trapezoidal cross-sectional shape, Int. J. Therm. Sci. 45 (2006) 1021–1026.
[29] S.W. Perng, H.W. Wu, A three-dimensional numerical investigation of trapezoid baffles effect on non-isothermal reactant transport and cell net power in a PEMFC, Appl. Energy 143 (2015) 81–95.
[30] L.S. Freire, E. Antolini, M. Linardi, E.I. Santiago, R.R. Passos, Influence of operational parameters on the performance of PEMFCs with serpentine flow field channels having different (rectangular and trapezoidal) cross-section shape, Int. J. Hydrogen Energy 39 (2014) 12052–12060.
[31] S. Ge, C.Y. Wang, Liquid water formation and transport in the PEFC anode, J. Electrochem. Soc. 154 (2007) 998–1005.
[32] J.M. Sergi, S.G. Kandlikar, Quantification and characterization of water coverage in PEMFC gas channels using simultaneous anode and cathode visualization and image processing, Int. J. Hydrogen Energy 36 (2011) 12381–12392.
[33] D. Lee, J. Bae, Visualization of flooding in a single cell and stacks by using a newly-designed transparent PEMFC, Int. J. Hydrogen Energy 37 (2012) 422–435.
[34] E. Carcadea, M.S. Ismail, D. BinIngham, L. Patularu, et al., Effects of geometrical dimensions of flow channels of a large-active-area PEM fuel cell: a CFD study, Int. J. Hydrogen Energy 46 (2021) 13572–13582.
[35] T. Wilberforce, F.N. Khatib, O.S. Ijaodola, E. Ogungbemi, et al., Numerical modelling and CFD simulation of a polymer electrolyte membrane (PEM) fuel cell flow channel using an open pore cellular foam material, Sci. Total Environ. 678 (2019) 728–740.
[36] J-Paul Kone, X. Zhang, Y. Yan, G. Hu, G. Ahmadi, CFD modeling and simulation of PEM fuel cell using OpenFOAM, Energy Proc. 145 (2018) 64–69.
[37] P. Barnoon, Numerical assessment of heat transfer and mixing quality of a hybrid nanofluid in a microchannel equipped with a dual mixer, Int J of Thermofluids 12 (2021) 100111.
[38] A. Iranzo, P. Boillat, CFD simulation of the transient gas transport in a PEM fuel cell cathode during AC impedance testing considering liquid water effects, Energy 158 (2018) 449–457.
[39] A. Solati, B. Nasiri, A. Mohammadi-Ahmar, K. Mohammadi, A.H. Safari, Numerical investigation of the effect of different layers configurations on the performance of radial PEM fuel cells, Renew. Energy 143 (2019) 1877–1889.
[40] C. Martínez Baca, R. Travis, M. Bang, Three-dimensional, single-phase, non-isothermal CFD model of a PEM fuel cell, J. Power Sources 178 (2008) 269–281.
[41] L. Wang, A. Husar, Z. Tianhong, L. Hongtan, A parametric study of PEMFC performances, Int. J. Hydrogen Energy 28 (2003) pp1263–1272.
[42] Q. Yan, H. Toghiani, H. Causey, Steady state and dynamic performance of proton exchange membrane fuel cells (PEMFCs) under various operating conditions and load changes, J Power Sourc 161 (2006) 492–502.
[43] Y. Yang, H. Jia, Z. Liu, N. Bai, et al., Overall and local effects of operating parameters on water management and performance of open-cathode PEM fuel cells, Applied Energ 315 (2022) 118978.
[44] X. Chen, J. Xu, Y. Fang, W. Li, et al., Temperature and humidity management of PEM fuel cell power system using multi-input and multi-output fuzzy method, Applied Therm Eng 203 (2022) 117865.
[45] C. Chan, N. Zamel, X. Li, J. Shen, Experimental measurement of effective diffusion coefficient of gas diffusion layer/microporous layer in PEM fuel cells, Electrochim. Acta 65 (2012) 13–21.
[46] M. Prokop, P. Capek, M. Vesely, M. Paidar, K. Bouzek, High-temperature PEM fuel cell electrode catalyst layers Part 2: experimental validation of its effective transport properties, Electrochim. Acta 413 (2022) 140121.
[47] P. Barnoon, D. Toghraie, B. Mehmandosut, M.A. Fazilati, S.A. Eftekhari, An agglomerate model for evaluating the electrochemical and hydrodynamic characteristics of a proton exchange membrane fuel cell, Journal of Simulation and Analysis of Novel Technologies in Mechanical Engineering 13 (3) (2021) 5–12.
[48] J. O. CeballosL. C. OrdoñezJ. M. Sierra, Numerical simulation of a PEM fuel cell: Effect of tortuosity parameters on the construction of polarization curves, Int. J. Hydrogen Energy, https://doi.org/10.1016/j.ijhydene.2022.03.112.
[49] M Arif, Sherman C. P. Cheung, J Andrews, Numerical investigation of effects of different flow channel configurations on the 100 cm2 PEM fuel cell performance under different operating conditions, Catal. Today, https://doi.org/10.1016/j.cattod.2021.07.016.
[50] A.A. EbrahimzadehI, KhazaeeA. Fasihfar, Numerical investigation of dimensions and arrangement of obstacle on the performance of PEM fuel cell, Heliyon 4 (11) (2018) e00974.
[51] T. DingX, BiD.P. Wilkinson, Numerical investigation of the impact of two-phase flow maldistribution on PEM fuel cell performance, Int. J. Hydrogen Energy 39 (2014) 469–480.